Biomedicine & Pharmacotherapy 192 (2025) 118620

Contents lists available at ScienceDirect

Biomedicine & Pharmacotherapy

journal homepage: www.elsevier.com/locate/biopha

Autophagy inhibition enhances sensitivity of alpelisib in PI3K–mutated non-small cell lung cancer

Jinyoung Kim [a,b,c,1], Chandani Shrestha [a,b,1], Tae Woo Kim [d], Sang-Bin Lee [a,b], Gwangbin Lee [a,b], Dasom Jung [a,b], Min Hwang [a,b], Shinwon Kang [e,f], Hyung Soon Park [g], Hyunho Kim [g], Ho Jung An [g], Dongwoo Chae [h,*], Byoung Yong Shim [g,*], Jiyoon Kim [a,b,c,**]

[a] Department of Pharmacology, College of Medicine, The Catholic University of Korea, Seoul 06591, Republic of Korea
[b] Department of Medical Sciences, Graduate School, The Catholic University of Korea, Seoul 06591, Republic of Korea
[c] Institute for Aging and Metabolic Diseases, College of Medicine, The Catholic University of Korea, Seoul 06591, Republic of Korea
[d] Department of Biopharmaceutical Engineering, Dongguk University-WISE, Gyeongju 38066, Republic of Korea
[e] Department of Physiology, University of Toronto, Toronto M5S 1A1, Canada
[f] Lunenfeld-Tanenbaum Research Institute, Mount Sinai Hospital, Sinai Health System, Toronto M5S 1A1, Canada
[g] Division of Oncology, Department of Internal Medicine, St. Vincent's Hospital, College of Medicine, The Catholic University of Korea, Suwon 16247, Republic of Korea
[h] Department of Pharmacology, Yonsei University College of Medicine, Seoul 03722, Republic of Korea

ARTICLE INFO

Keywords:
Alpelisib
Autophagy
Chloroquine
EGFR
NSCLC
PI3K

ABSTRACT

Non-small cell lung cancer (NSCLC) is a prevalent and lethal form of lung cancer with few effective treatment options, and targeted therapies for PI3K–mutated NSCLC remain particularly limited. The phosphatidylinositol 3-kinase (PI3K) pathway, frequently activated in NSCLC, is a viable therapeutic target, especially in tumors harboring PI3K mutations. Alpelisib (BYL719), a selective PI3Kα inhibitor, has shown promise, but its efficacy is often hampered by compensatory survival mechanisms, including autophagy. This study assesses the therapeutic potential of alpelisib as a monotherapy and in combination with an autophagy inhibitor for PI3K–mutated NSCLC. Alpelisib significantly reduced cell viability in human NSCLC cell lines in a dose- and time-dependent manner, with enhanced markers of autophagy and apoptosis, with pronounced effects in PI3K–mutant H460 cells. Co-treatment with alpelisib and chloroquine (CQ) further suppressed tumor cell growth, viability, migration, and colony formation more effectively than alpelisib alone, owing to increased apoptosis, elevated early and late apoptotic populations, and increased levels of cleaved PARP and caspase-3. In xenograft mouse models, the combination of alpelisib and CQ significantly inhibited tumor growth and reduced EGFR-Ras signaling compared to monotherapy. These findings suggest that combining alpelisib with autophagy inhibition significantly enhances its antitumor activity in PI3K–mutated NSCLC, highlighting a promising therapeutic strategy to address unmet clinical needs in this molecular subset. This discovery opens new possibilities for developing innovative targeted therapies for challenging NSCLC.

1. Introduction

Lung cancer remains one of the leading causes of cancer-related mortality worldwide, accounting for approximately 1.8 million deaths in 2022 [1]. This malignancy is particularly challenging due to its aggressive nature and poor prognosis, with a five-year survival rate of only 5 % for patients with advanced disease [2]. Lung cancer is broadly categorized into small cell lung cancer and non-small cell lung cancer (NSCLC), and about 85 % of all lung cancer cases are NSCLC. Current treatment options for NSCLC are inadequate, underscoring the critical need for innovative therapeutic approaches to improve patient outcomes [3].

One of the key pathways implicated in the progression and survival of NSCLC is the phosphatidylinositol 3-kinase (PI3K) pathway. Aberrant activation of this pathway, often due to PIK3CA mutations, has been observed in a significant subset of NSCLC cases, leading to enhanced

* Corresponding authors.
** Corresponding author at: Department of Pharmacology, College of Medicine, The Catholic University of Korea, Seoul 06591, Republic of Korea.
E-mail addresses: dongy@yuhs.ac (D. Chae), shimby@catholic.ac.kr (B.Y. Shim), jykim@catholic.ac.kr (J. Kim).
[1] These authors contributed equally to this work.

https://doi.org/10.1016/j.biopha.2025.118620
Received 17 July 2025; Received in revised form 24 September 2025; Accepted 1 October 2025
Available online 2 October 2025

tumor growth, survival, and resistance to apoptosis [4,5]. Previous research has demonstrated that inhibiting the PI3K pathway can effectively hinder the growth and invasion of cancer cells reliant on PI3K, such as NSCLC [6,7]. Consequently, the inhibition of class I PI3Ks is a promising therapeutic strategy, and specific PI3K inhibitors have been approved to treat several cancer types.

Alpelisib, an isoform-specific inhibitor targeting PI3K–alpha, received FDA approval in 2019 for the treatment of advanced or metastatic breast cancer with PI3K mutations [8]. While monotherapy with isoform-specific PI3K inhibitors has shown limited effectiveness in early-phase trials, recent evaluations of alpelisib in combination with olaparib have yielded promising results in patients with ovarian cancer or triple-negative breast cancer [9]. Additionally, alpelisib has enhanced the antitumor effect of paclitaxel in PI3K–mutated human gastric cancer models [10]. These positive results warrant further exploration of alpelisib as a single or combination therapy across different cancer subtypes with PI3K mutations.

Although multiple PI3K inhibitors, including pictilisib, buparlisib, and alpelisib, have been evaluated in NSCLC, clinical activity has generally been modest, with low response rates and frequent emergence of resistance [11–13]. A key adaptive mechanism is therapy-induced cytoprotective autophagy, which attenuates the cytotoxic effects of PI3K pathway blockade. Accordingly, combining PI3K inhibitors with autophagy inhibition has emerged as a rational strategy. Among clinically used autophagy inhibitors, chloroquine (CQ) and hydroxychloroquine (HCQ) inhibit lysosomal acidification and disrupt autophagosome–lysosome fusion [14,15]. Notably, preclinical studies show that CQ potentiates the antitumor efficacy of both chemotherapy and targeted agents in NSCLC and other tumor models [16,17]. Given its clinical availability, safety profile, and supportive preclinical evidence, CQ was selected as the autophagy inhibitor to combine with alpelisib in this study.

Autophagy is a cellular process that can promote tumor cell survival under therapeutic stress by degrading and recycling cellular components. Inhibiting autophagy has been shown to enhance the antitumor effects of various chemotherapeutic agents. Therefore, combining PI3K inhibitors with autophagy inhibitors might potentiate their therapeutic efficacy against NSCLC [18–20]. For this study, we conducted *in vitro* and *in vivo* experiments to investigate the combined effects of alpelisib and autophagy inhibitors on NSCLC.

2. Materials and methods

2.1. Cell lines

The A549 and H460 human NSCLC cell lines were purchased from the Korea Cell Line Bank (KCLB, Seoul, Republic of Korea). All cell lines were maintained in RPMI-1640 medium (Gibco, Grand Island, NY, USA), supplemented with 10 % fetal bovine serum (Gibco), 100 U/mL of penicillin, and 100 mg/mL of streptomycin (Gibco). All cells were incubated in sterile conditions at 37°C and 5 % CO_2. Mycoplasma contamination was tested and confirmed negative using a MycoStrip™ mycoplasma detection kit (InvivoGen, San Diego, CA, USA).

2.2. Cell viability assay

Cell viability was assessed using Cell Counting Kit-8 (CCK-8) reagent (Dojindo Laboratories, Kumamoto, Japan, CK04) according to the manufacturer's instructions. Human NSCLC cells were seeded into 96-well plates at a density of 5×10^3 cells per well and allowed to attach overnight. Treatment with various concentrations of alpelisib (BYL719) and/or other autophagy inhibitors was then applied, and cells were incubated for 4, 8, 24, and 48 h. After treatment, 10 μl of CCK-8 reagent was added to each well, and the plates were incubated with at 37 °C for 1 h. The absorbance was measured at 450 nm using a microplate spectrophotometer (BioTek, Winooski, VT, USA). The percentage of cell viability was calculated relative to vehicle-treated control wells. For each cell line, the half-maximal inhibitory concentration (IC_{50}) of BYL719 was obtained from dose–response curves as the concentration that reduced viability to 50 % of the control.

2.3. Synergy evaluation by combination index (CI) analysis

Drug interactions were evaluated using CCK-8 viability data after treatment with BYL719, CQ, or their fixed-ratio combinations in A549 and H460 cells. The combination index (CI) was computed with CompuSyn (ComboSyn, Inc., Paramus, NJ, USA), which implements the median-effect principle and the unified Chou–Talalay method [21]. For each condition, the fraction affected (Fa) was defined as:

$Fa = 1 -$ (absorbance of treated wells / absorbance of control wells)

CI values were generated by the software based on the Chou–Talalay algorithm and plotted against Fa (CI on the y-axis, Fa on the x-axis). Interaction was interpreted as follows: $CI < 1$, synergy; $CI = 1$, additivity; $CI > 1$, antagonism.

2.4. Immunoblot analysis

Cell and tissue lysates were prepared using lysis buffer (20 mM Tris-HCl, pH 7.9, 150 mM NaCl, 2 mM EDTA, 5 mM EGTA, 5 % glycerol, 1 % Triton X-100) supplemented with Protease Inhibitor Cocktail (Roche, Basel, Switzerland), 1 mM phenylmethanesulfonyl-fluoride, 10 mM NaF, and 1 mM Na_3VO_4, and then they were subjected to sonication. The protein concentration in each sample was determined using a Bradford assay. Equal amounts of protein were separated by SDS-PAGE on 5–12 % polyacrylamide gels (LABIS KOMA, Seoul, Korea, KG5012) and transferred to nitrocellulose membranes (Merk Millipore, Burlington, MA, USA). The membranes were then blocked using either 5 % milk or 5 % BSA and allowed to incubate with primary antibodies against p62/SQSTM1 (Progen, GP62-C, 1:1000 dilution), LC3A/B (Cell Signaling Technology, 4108, 1:1000 dilution), PARP (Cell Signaling Technology, 9532, 1:1000 dilution), cleaved caspase-3 (CASP3; Cell Signaling Technology, 9662, 1:1000 dilution), phospho-mTOR (Ser2448) (Cell Signaling Technology, 2971, 1:1000 dilution), mTOR (Cell Signaling Technology, 2972, 1:1000 dilution), phospho-AKT (Ser474) (Cell Signaling Technology, 8599, 1:1000 dilution), AKT (Cell Signaling Technology, 2964, 1:1000 dilution), phospho-STAT3 (Tyr705) (Cell Signaling Technology, 9131, 1:1000 dilution), STAT3 (Cell Signaling Technology, 12640, 1:1000 dilution), beclin-1 (BECN1; Cell Signaling Technology, 3495, 1:1000 dilution), ATG7 (Cell Signaling Technology, 8558, 1:1000 dilution), ATG5 (Cell Signaling Technology, 2630, 1:1000 dilution), phospho-EGF receptor (Tyr1068) (Cell Signaling Technology, 3777, 1:1000 dilution), EGF receptor (EGFR; Cell Signaling Technology, 2232, 1:1000 dilution), PI3 kinase (PI3K; Cell Signaling Technology, 4249, 1:1000 dilution), Ras (Cell Signaling Technology, 8955, 1:1000 dilution), phosphor-RAF1 (S259) (Abnova, PAB25227, 1:1000 dilution), RAF1 (Abnova, PAB18217, 1:1000 dilution), phosphor-MEK1/2 (Ser217, Ser221) (Cell Signaling Technology, 9154, 1:1000 dilution), MEK1/2 (Cell Signaling Technology, 9122, 1:1000 dilution), phosphor-ERK1/2 (Thr202, Tyr204) (Cell Signaling Technology, 4370, 1:1000 dilution), ERK1/2 (Cell Signaling Technology, 4695, 1:1000 dilution), BiP (Cell Signaling Technology, 3177, 1:1000 dilution), CHOP (Cell Signaling Technology, 2895, 1:1000 dilution), or β-actin (ACTB; Abcam, ab8227, 1:2000 dilution) overnight at 4°C. After the membranes were incubated with HRP-conjugated secondary antibodies (Invitrogen, 31460 or 31430) for 1 h, immunoreactive protein bands were visualized using a D-Plus™ ECL Femto system (Dongin Biotech, Seoul, Korea, ECL-FS100) and a LAS-4000 mini system (Fujifilm, Tokyo, Japan). Densitometry of the protein bands was performed using ImageJ (NIH).

2.5. mRFP-GFP-LC3 assay

Autophagic flux was evaluated using the tandem *mRFP–GFP–LC3*

construct (ptfLC3; Addgene #21074). Human NSCLC cells were transfected with the plasmid using Lipofectamine™ 3000 (Thermo Fisher Scientific, L3000015) according to the manufacturer's instructions. Twenty-four hours post-transfection, cells were treated with BYL719 and/or CQ for an additional 24 h. Confocal imaging was performed on an LSM 780 microscope (Zeiss, Oberkochen, Germany). GFP and RFP signals were acquired, and puncta were defined as non-nuclear fluorescent punctate structures on a dark background. Yellow puncta (GFP + RFP) were classified as autophagosomes, whereas red-only puncta (RFP) represented autolysosomes. For each condition, yellow and red puncta were quantified in > 40 cells to assess autophagic flux (reported as puncta per cell).

2.6. Wound healing assay

To evaluate the migration ability of A549 and H460 cells, a wound healing assay was conducted. The cells were seeded in 12-well plates at a density of 2×10^6 cells per well and incubated until a confluent monolayer was established. A 10 μl pipette tip was used to create a long, thin scratch, generating an acellular area. The cells were then incubated in media containing BYL719 and/or CQ. The width of the wound was observed at 0 and 24 h using an IX73 microscope (Olympus, Tokyo, Japan), and the area of wound closure was measured using ImageJ software (NIH, Bethesda, MD, USA).

2.7. Clonogenic assay

For the clonogenic assay, also known as the colony formation assay, cell suspensions were plated at a density of 1000 cells per well in 6-well plates and incubated overnight. The cells were then treated with BYL719 and/or CQ for 10 days. After 10 days, the colonies were fixed with 4 % paraformaldehyde for 15 min at room temperature and then stained with 0.5 % crystal violet (Sigma, St. Louis, MO, USA, C0775) for 20 min. Stereoscopic imaging was performed using an SMZ745T microscope (Nikon, Tokyo, Japan), and the area and number of colonies were evaluated using ImageJ software (NIH).

2.8. Annexin V-FITC/PI apoptosis assay

Apoptotic cells were detected using an Annexin V-FITC/PI apoptosis detection kit (BD Biosciences, San Jose, CA, USA, 556547) according to the manufacturer's instructions. A549 and H460 cells were seeded in 6-well plates at a density of 2×10^5 cells per well and treated with BYL719 and/or CQ for 24 h. After they were harvested, the cells were resuspended in a binding buffer consisting of 10 mM HEPES/NaOH (pH 7.4), 140 mM NaCl, and 25 mM $CaCl_2$. Fluorescein isothiocyanate (FITC)-conjugated Annexin V (Annexin V-FITC) and propidium iodide (PI) staining was performed for 15 min, and the samples were analyzed using a FACS Canto flow cytometer (BD Biosciences, San Jose, CA, USA).

2.9. Mouse xenograft and drug treatment

Five-week-old male BALB/c nude mice were purchased from Orient Bio (Seongnam, Korea). The mice were housed under controlled conditions at a temperature of 22 ± 2 °C, 60 % humidity, and a 12-h light/dark cycle, with *ad libitum* access to food and water. To investigate whether the combined administration of BYL719and CQ synergistically suppresses tumor growth in a xenograft mouse model, 6-week-old male BALB/c nude mice were subcutaneously inoculated in the right flank with 100 □l of a mixture (1:1 Matrigel and medium) containing A549 cells (5.0×10^6) or H460 cells (5.0×10^6). When the tumors reached approximately 100 mm^3, the mice were randomly divided into four groups (n = 5 per group): (1) vehicle (Veh)-treated control group (daily intraperitoneal [i.p.] injection), (2) BYL719-treated group (25 mg/kg, daily i.p. injection), (3) CQ-treated group (30 mg/kg, daily i.p. injection), and (4) BYL719 +CQ co-treated group (daily i.p. injection). Tumor size was measured three times a week using a digital Vernier caliper (Mitutoyo, Kawasaki, Japan), and tumor volume was calculated using the formula for ellipsoidal volume: $V = (\text{length} \times \text{width}^2)/2$. After the final measurement, the tumors were collected for further analysis.

All animals were maintained in an SPF facility accredited by the Association for the Assessment and Accreditation of Laboratory Animal Care International. All animal experiments were approved by the Institutional Animal Care and Use Committee (IACUC) of the Catholic University of Korea and were conducted in accordance with IACUC guidelines (Approval number: CUMS-2022–0037–10).

2.10. Statistical analysis

All data are represented as the mean ± SEM for experiments using cell lines and the mean ± SD for experiments using mice, as noted in the figure legends. Statistical significance was tested using one-way or two-way ANOVA, as noted in the figure legends. P values less than 0.05 were considered to indicate statistically significant differences ($^*p < 0.05$, $^{**}p < 0.01$, and $^{***}p < 0.001$). Graph generation and statistical analyses were performed using GraphPad Prism 8.0 software (GraphPad Software Inc., San Diego, CA, USA).

3. Results

3.1. Alpelisib in combination with chloroquine, an autophagy inhibitor, synergistically suppresses human NSCLC cell growth

Alpelisib, a PI3K inhibitor, has demonstrated potential in inhibiting tumor growth in various cancers by targeting the PI3K/AKT/mTOR pathway, which plays a crucial role in cell survival, proliferation, and apoptosis [2,22]. However, its specific effects on NSCLC cells and the underlying mechanisms remain to be fully elucidated. To address this, we investigated the antitumor effects of alpelisib in combination with various autophagy inhibitors using two genetically distinct NSCLC cell lines, A549 and H460. A549 cell line contains a KRAS mutation and is wild-type for EGFR, whereas H460 cell line harbors co-occurring mutations in KRAS and the PI3K pathway, rendering these models appropriate for evaluating PI3K–targeted therapies [23,24]. These cell lines were treated with various doses of alpelisib for 4, 8, 24, and 48 h, and cell viability was assessed. A dose-dependent reduction in cell viability was observed in both cell lines, with the effect becoming more pronounced at longer treatment durations at the same concentration (Fig. S1A and B). To assess alpelisib sensitivity, 24-h IC_{50} values were determined in A549 and H460 cells. The IC_{50} was 39.67 μM (95 % CI, 30.67–51.22) in A549 and 50.16 μM (95 % CI, 40.94–61.54) in H460 (Fig. S1C and D). Based on these estimates, 30 and 60 μM were used in subsequent experiments to probe effects near the IC_{50} and to facilitate detection of potential synergy with CQ without inducing near-maximal cytotoxicity. Previous studies have demonstrated that PI3K inhibition can induce autophagy, an adaptive cellular response often exploited by tumor cells to overcome therapeutic and metabolic stress [25,26]. Based on this, we hypothesized that autophagy inhibition could potentiate the antitumor efficacy of alpelisib in A549 and H460 cells. Thus, we investigated the combined treatment of alpelisib with various autophagy inhibitors. Co-treatment with alpelisib and five autophagy inhibitors (3-methyladenine [3-MA], wortmannin [Wort], chloroquine [CQ], hydroxychloroquine [HCQ], and bafilomycin A1 [BafA]) demonstrated a distinct antitumor effect in A549 and H460 cells compared to alpelisib alone (Fig. 1A and B). Specifically, co-treatment with alpelisib and either 3-MA or CQ significantly reduced cell viability in A549 and H460 cells compared to alpelisib treatment alone, with the pronounced effect in H460, indicating preferential sensitivity of PI3K–mutant cells (Fig. 1A and B). Since these inhibitors target different stages of autophagy—3-MA at initiation and CQ at lysosomal fusion—they were selected for further mechanistic studies. Immunoblot analysis demonstrated that 3-MA treatment decreased the conversion of LC3-I to

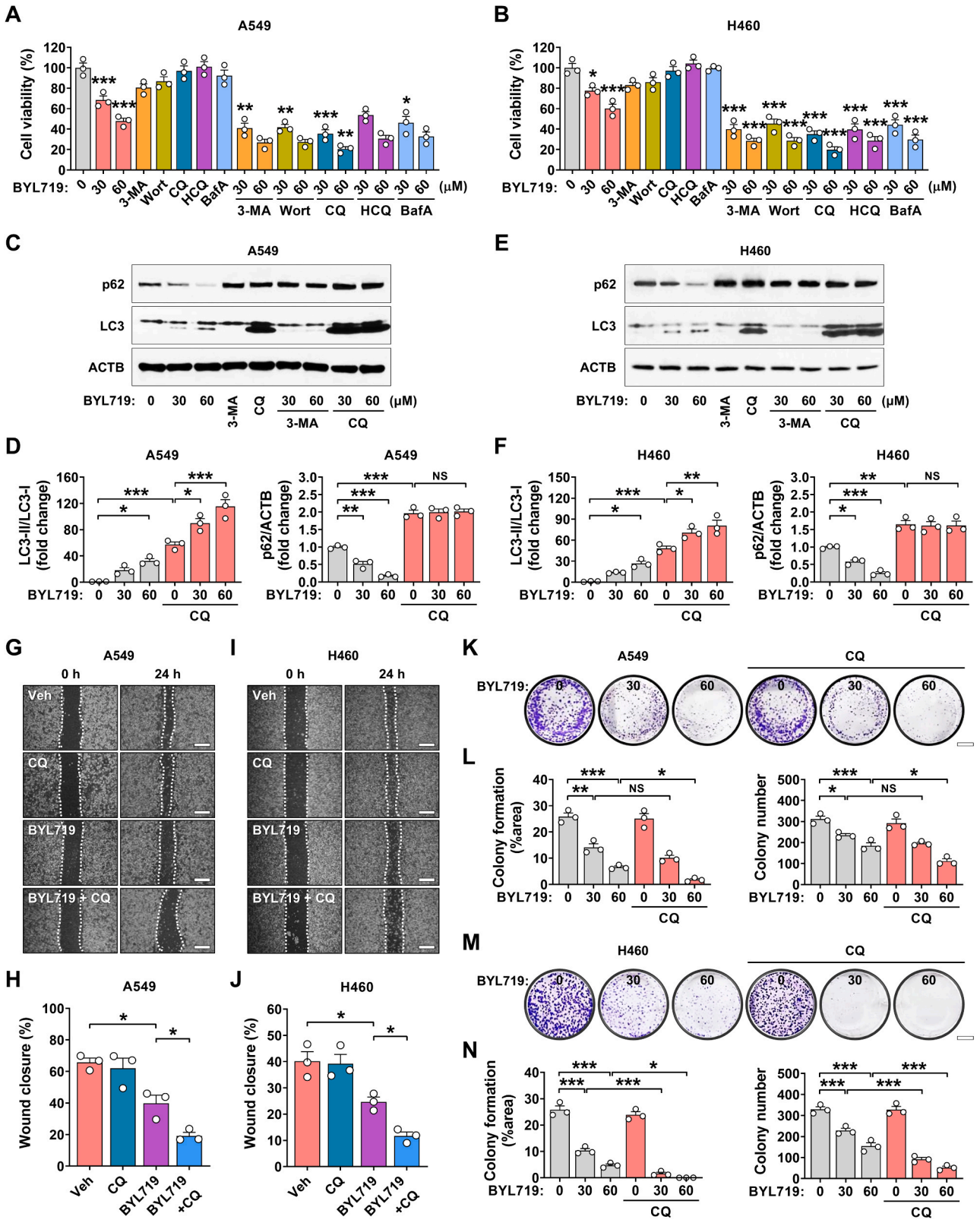

Fig. 1. Alpelisib combined with an autophagy inhibitor synergistically suppresses human NSCLC cell growth. A–B Relative viability of A549 (A) and H460 (B) cells treated with alpelisib (BYL719) in the absence and presence of each autophagy inhibitor: 3-MA (1 mM), wortmannin (Wort; 5 μM), chloroquine (CQ; 50 μM), hydroxychloroquine (HCQ; 5 μM), bafilomycin A1 (BafA; 50 nM). C–F Immunoblotting analysis of autophagy markers (p62 and LC3) in A549 (C) and H460 (E) cells treated with BYL719 in the absence and presence of each autophagy inhibitor. The densitometric analyses are summarized in (D and F). Band intensity was determined by densitometry and normalized to LC3-I for LC3-II and β-actin (ACTB) for p62. G–J Wound healing assay in A549 (G) and H460 (I) cells treated with BYL719 in the absence and presence of CQ. Scale bar, 300 μm. The quantitative analyses are summarized in (H and J). K–N Colony formation assay in A549 (K) and H460 (M) cells treated with BYL719 in the absence and presence of CQ. Scale bar, 5 mm. The quantitative analyses are summarized in (L and N). All data are shown as the mean ± SEM. *p < 0.05, **p < 0.01, and ***p < 0.001 by two-way ANOVA with Tukey's test.

LC3-II, consistent with early-stage autophagy inhibition, while CQ treatment led to LC3-II accumulation, indicative of late-stage autophagy blockade (Fig. 1C–F; Fig. S2A and B). The ratio of LC3-II to LC3-I band intensity revealed that co-treatment with CQ significantly increased the accumulation of LC3-II in A549 and H460 cells compared to alpelisib treatment alone, confirming that alpelisib induces autophagy (Fig. 1C–F). Consistent with these findings, tandem mRFP–GFP–LC3 imaging showed an alpelisib dose-dependent increase in LC3 puncta, and co-treatment with CQ further elevated the accumulation of LC3-lipidated autophagosomes in both A549 and H460 cells. Because CQ inhibits autophagosome–lysosome fusion, this accumulation is consistent with alpelisib-induced activation of autophagic flux (Fig. S3A–D). Additionally, levels of cleaved caspase-3 (c-CASP3) were markedly higher in A549 and H460 cells co-treated with CQ compared to those treated with alpelisib alone, these levels were notably higher than in cells co-treated with 3-MA, suggesting that inhibition of late-stage autophagy more effectively enhances alpelisib-induced apoptosis (Fig. 1C–F; Fig. S2A and B). Among the various autophagy inhibitors tested, CQ had the best therapeutic efficacy without increasing toxicity, and it has been approved for other diseases, such as malaria, which facilitates its potential application in human studies [27]. Therefore, CQ was selected as the combination therapy option for the subsequent studies. Subsequently, synergy between alpelisib and CQ was evaluated by the Chou–Talalay method. The combination index (CI) was < 1 across a range of alpelisib–CQ dose combinations in both A549 and H460 cells, indicating robust synergism (Fig. S4). These findings justified pursuing the combination in subsequent experiments and further supported our use of 30 and 60 μM alpelisib as working concentrations.

Next, we investigated the effect of co-treatment with alpelisib and CQ on NSCLC cell growth. Cell migration and colony formation are fundamental processes in tumorigenesis and metastasis [27]. The wound healing assay assesses cell migration by measuring the closure of a scratch or wound introduced to a cell monolayer [28]. Therefore, we conducted both wound healing and clonogenic assays in human NSCLC cells to evaluate how co-treatment with alpelisib and CQ affected migration ability and colony formation capacity. The extent of wound closure was notably reduced in alpelisib-treated A549 and H460 cells, compared with vehicle-treated cells, and a further significant reduction was observed in alpelisib and CQ, compared with alpelisib-treated cells (Fig. 1G–J). The clonogenic assay revealed that the area and number of colonies in alpelisib-treated A549 and H460 cells were significantly reduced, compared with vehicle-treated cells, and a further reduction was observed in cells co-treated with alpelisib and CQ, compared with alpelisib-treated cells (Fig. 1K–N). These results suggest that combination treatment with alpelisib and CQ produces greater reductions in migration and colony formation than alpelisib monotherapy.

3.2. Alpelisib in combination with CQ enhances PI3K–mutated human NSCLC cell death

To investigate the therapeutic effects of co-treatment with alpelisib and CQ in NSCLC cells, we focused on apoptosis using flow cytometry. The use of PI and Annexin V-FITC is a standard procedure for monitoring the progression of apoptosis. Early apoptotic cells are Annexin V-positive and PI-negative, and late (end-stage) apoptotic cells are Annexin V/PI-double-positive [29]. After Annexin V and PI staining, we observed that the number of both early (Annexin V-FITC$^+$/PI$^-$ population) and late apoptotic cells (Annexin V-FITC$^+$/PI$^+$ population) increased dose-dependently but not significantly in A549 and H460 cells after alpelisib treatment alone (Fig. 2A–D). Co-treatment with alpelisib and CQ significantly increased the proportions of early and late apoptotic cells in both A549 and H460 compared with the same dose of alpelisib alone, with a more pronounced increase in H460 than in A549 (Fig. 2A–D).

To further elucidate the mechanism underlying alpelisib–CQ–induced cell death, we performed tandem mRFP–GFP–LC3 imaging, which confirmed that alpelisib increases autophagic flux (Fig. S3A–D), consistent with the immunoblot data in Fig. 1C–F. In contrast, CQ blocks autophagosome degradation by impairing autophagosome–lysosome fusion, thereby preventing lysosomal clearance of pro-apoptotic factors and promoting apoptosis. To corroborate these findings and assess a role for endoplasmic reticulum (ER) stress, we examined apoptotic (PARP, CASP3) and ER-stress (BiP, CHOP) markers by immunoblotting. Inhibition of autophagy with CQ heightened ER stress, evidenced by decreased BiP and increased CHOP (Fig. S3E–H). Notably, marked ER stress can be accompanied by reduced BiP, while CHOP promotes intrinsic apoptosis by shifting the balance of pro- and anti-apoptotic proteins, such as Bax and Bcl-2, toward caspase activation and cell death [30–32]. Consistent with these observations, levels of cleaved PARP and cleaved CASP3 increased with alpelisib treatment alone, but not significantly (Fig. 2E-H). However, co-treatment with alpelisib and CQ resulted in a significant increase in the levels of cleaved PARP and CASP3 compared to alpelisib alone (Fig. 2F and H). The induction of cleaved PARP and cleaved caspase-3 was most pronounced in H460 cells, consistent with the preferential efficacy of the combination in PI3K–mutant cells. Collectively, these results suggest that alpelisib and CQ combination therapy has synergistic effects in NSCLC cells that promote apoptosis, with preferential activity in PI3K–mutant H460 cells. Mechanistically, alpelisib-induced enhancement of autophagic flux, together with CQ-mediated blockade of autophagosome degradation and consequent ER stress, converges to drive synergistic activation of apoptosis.

3.3. Alpelisib treatment combined with CQ inhibits EGFR-Ras signaling in PI3K–mutated NSCLC cells

To comprehensively understand the pathways and mechanisms involved in the co-treatment with alpelisib and CQ in NSCLC cells, we analyzed the expression of proteins associated with the PI3K/AKT/mTOR pathway, autophagy, and tumorigenesis. First, we assessed the expression of key autophagy-related proteins following alpelisib treatment. Immunoblot analysis demonstrated a significant decrease in the expression of phosphorylated mTOR and p62, coupled with an increase in LC3 expression, indicating autophagy activation in response to alpelisib treatment. Interestingly, the expression of other proteins remained unchanged, suggesting a specific effect on autophagy-related markers (Fig. 3A–D). Next, we explored the impact of alpelisib on the PI3K/AKT/mTOR signaling pathway, a pivotal pathway implicated in cancer progression. Immunoblot analysis revealed a marked reduction in phosphorylated AKT and phosphorylated mTOR expression following alpelisib treatment, indicative of pathway inhibition (Fig. 3A–D). Notably, total AKT protein expression decreased, particularly in H460 cells, underlining the dose-dependent effect of alpelisib, either alone or in combination with CQ (Fig. 3A–D). We next interrogated EGFR effector pathways implicated in survival and proliferation—PI3K/AKT/mTOR, RAS/ERK, and JAK/STAT3. Alpelisib significantly decreased STAT3 phosphorylation at Tyr705 (p-STAT3 Y705) in both A549 and H460 cells (Fig. 3A–D). However, addition of CQ did not further reduce p-STAT3, indicating that JAK/STAT3 signaling was not synergistically modulated by the combination. Additionally, we examined the effects of alpelisib and CQ combination therapy on the epidermal growth factor receptor (EGFR) and Ras signaling pathways, crucial players in tumor progression [33]. Alpelisib monotherapy significantly decreased p-EGFR (Y1068) in both A549 and H460 cells, and this suppression was further enhanced by co-treatment with CQ (Fig. 3C and D). In contrast, reductions in total EGFR and total Ras were prominent under the combination in H460 cells harboring a *PIK3CA* mutation, whereas KRAS-mutant A549 cells showed only modest changes (Fig. 3C and D). Thus, although p-EGFR signaling was suppressed in both lines, downregulation of total EGFR and Ras was preferentially observed in the PI3K–mutant background.

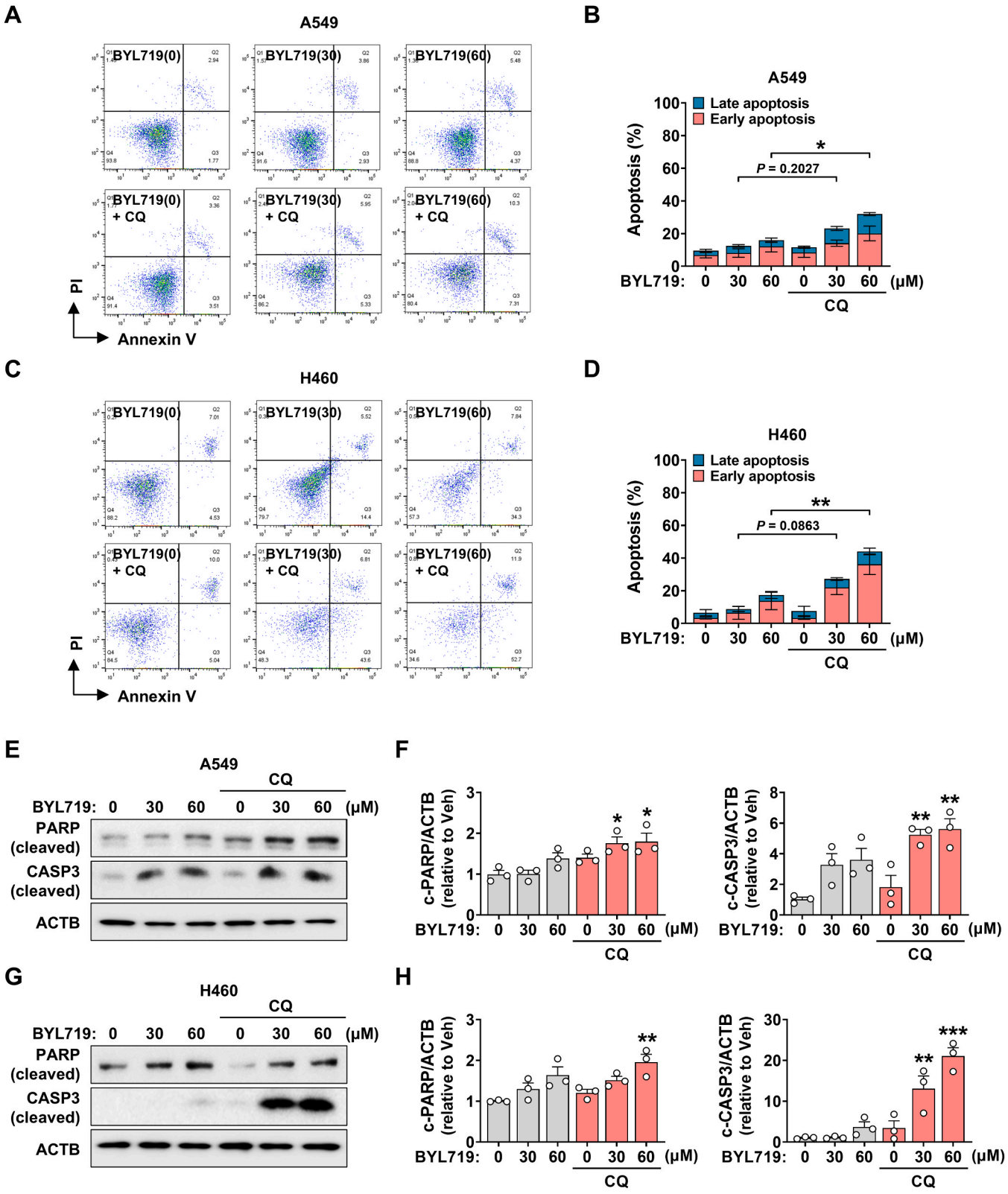

Fig. 2. Alpelisib combined with chloroquine synergistically enhances apoptosis in human NSCLC cells. A–D Flow cytometry analysis of apoptosis in human A549 (A) and H460 (C) cells treated with alpelisib (BYL719) in the absence and presence of chloroquine (CQ; 50 μM). The quantitative analyses are summarized in (B and D). E–H Immunoblotting analysis of apoptosis-related proteins (PARP and cleaved caspase-3) in A549 (E) and H460 (G) cells treated with BYL719 in the absence and presence of CQ. The quantitative analyses are summarized in (F and H). Band intensity was determined by densitometry and normalized to β-actin (ACTB) band intensity. All data are shown as the mean ± SEM. *$p < 0.05$, **$p < 0.01$, and ***$p < 0.001$ by two-way ANOVA (B and D) and one-way ANOVA (F and H) with Tukey's test.

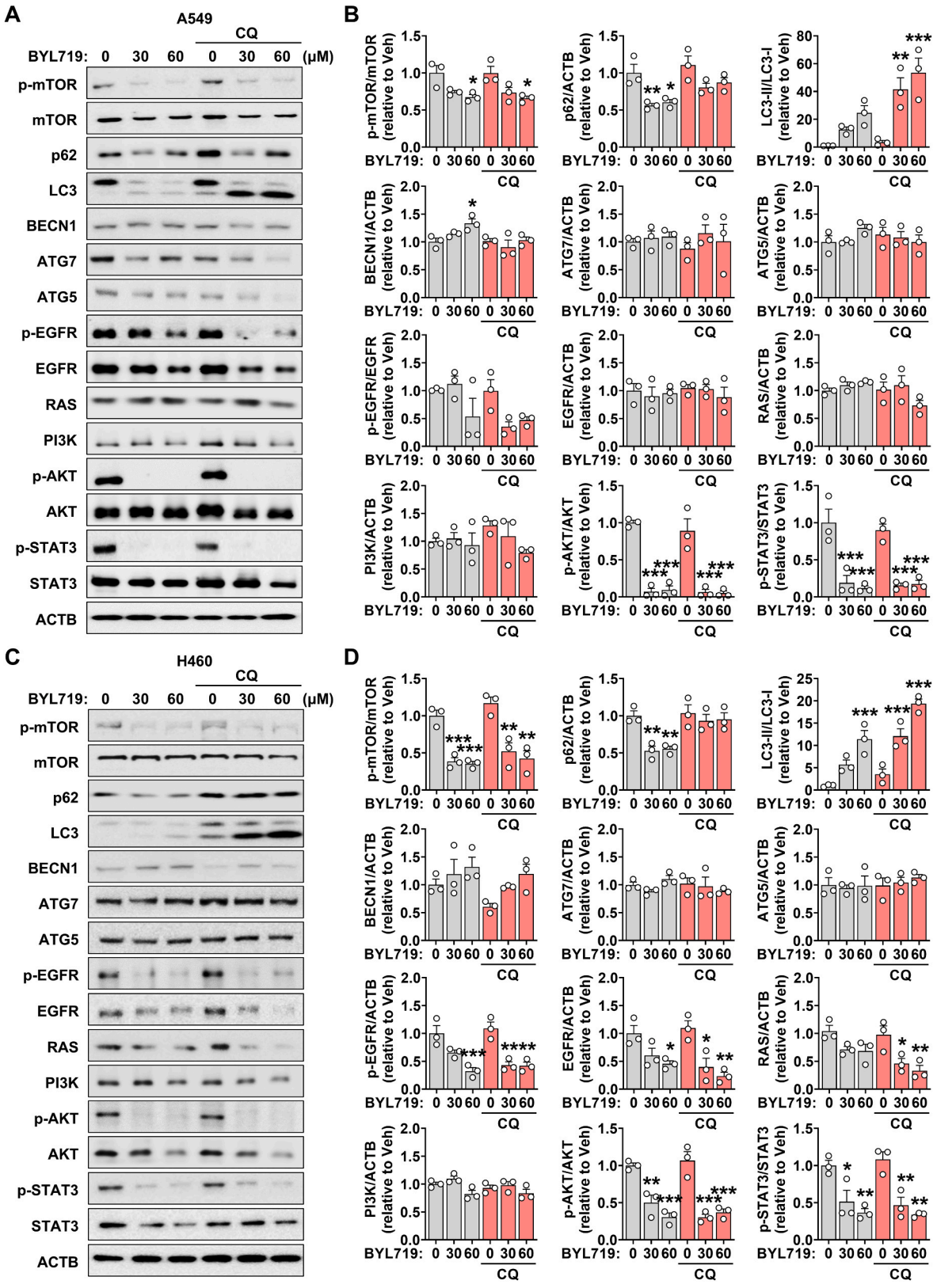

Fig. 3. Alpelisib combined with chloroquine reduces the expression of EGFR and Ras in PI3K–mutated NSCLC cells. A–D Immunoblotting analysis of autophagy (p62, LC3, ATG5, and ATG7), the PI3K/AKT/mTOR pathway (PI3K, p-AKT, and p-mTOR), and tumorigenesis (p-EGFR, RAS, and p-STAT3) in A549 (A) and H460 (C) cells treated with alpelisib (BYL719) in the absence and presence of chloroquine (CQ; 50 μM). The quantitative analyses are summarized in (B and D). Band intensity was determined by densitometry and normalized to β-actin (ACTB) band intensity. All data are shown as the mean ± SEM. *$p < 0.05$, **$p < 0.01$, and ***$p < 0.001$ by one-way ANOVA with Tukey's test.

Recently, a mechanistic computational model was developed to elucidate the complexity of the PI3K signaling network. This model proposed that there is negative crosstalk between the PI3K/AKT/mTOR signaling pathway and the Raf/MEK/ERK signaling pathway, with the Raf/MEK/ERK pathway exerting negative feedback regulation on the upstream epidermal growth factor receptor (EGFR) and Ras [34]. Consequently, we investigated whether the downregulation of EGFR and Ras expression by alpelisib in NSCLC cells harboring PI3K mutations is associated with the Raf/MEK/ERK signaling pathway. Immunoblot analysis demonstrated that the Raf/MEK/ERK pathway was upregulated following alpelisib treatment and was significantly further enhanced by co-treatment with CQ (Fig. S5A and B). Furthermore, combined treatment with alpelisib and CQ resulted in a marked inhibition of EGFR and Ras expression, suggesting a potential negative feedback regulation of EGFR and Ras expression by the activated Raf/MEK/ERK signaling pathway (Fig. S5A and B). To test ERK dependence directly, H460 cells were treated with alpelisib and CQ in the presence or absence of the ERK inhibitor SCH772984. The alpelisib–CQ combination significantly increased ERK phosphorylation while reducing total EGFR and Ras protein levels. Notably, co-treatment with SCH772984 suppressed ERK phosphorylation and restored EGFR and Ras expression toward baseline (Fig. S5C and D). These results indicate that compensatory ERK activation contributes to EGFR and Ras downregulation, and that autophagy blockade amplifies this feedback, particularly in PI3K–mutant NSCLC cells.

3.4. Co-treatment of alpelisib and CQ strongly suppresses tumor growth and EGFR-Ras signaling in xenograft mouse models

Given the inhibition of cell growth and migration, along with enhanced cell death observed in NSCLC cells, we investigated whether combination treatment with alpelisib and CQ would synergistically suppress tumor growth in a xenograft mouse model. BALB/c nude mice were subcutaneously inoculated with human NSCLC cells (A549 or H460) and subsequently treated with vehicle (Veh; DMSO), alpelisib (BYL719; 25 mg/kg), chloroquine (CQ; 30 mg/kg), or a combination of alpelisib and chloroquine (BYL719 +CQ). Alpelisib was administered at 25 mg/kg and CQ at 30 mg/kg in mice. Using standard body-surface-area conversion (mouse → human, Km: 3/37) [35], these correspond to human-equivalent doses (HEDs) of approximately 2.0 mg/kg and 2.4 mg/kg, respectively (approximately 120 mg/day and 145 mg/day for a 60 kg adult). Clinically, alpelisib is typically given at 300 mg once daily, and CQ at 250–500 mg/day, depending on indication. Thus, while the alpelisib HED is below the approved clinical dose and the CQ HED falls within clinically used ranges, both are clinically achievable and do not constitute excessive exposure, supporting the translational relevance of the combination. The selected doses are also consistent with prior preclinical regimens demonstrating on-target inhibition and antitumor activity for alpelisib (25–50 mg/kg) and autophagy blockade by CQ in xenograft models [36]. Tumor size and weight were significantly reduced in alpelisib-treated mice with A549 or H460 xenografts, compared with Veh-treated mice, with a further significant reduction observed in PI3K–mutated H460 xenograft mice co-treated with alpelisib and CQ (Fig. 4A–D). Tumor growth inhibition was more pronounced in H460 xenografts than in A549 xenografts, consistent with preferential sensitivity of PI3K–mutant tumors. Notably, CQ monotherapy achieved approximately 30–40 % tumor growth inhibition, although this did not reach statistical significance. However, beyond autophagy blockade, CQ has been reported to modulate Toll-like receptor 9, p53, and CXCR4–CXCL12 signaling in cancer cells, as well as tumor vasculature, cancer-associated fibroblasts, and immune components within the stroma [37]. This suggests that CQ monotherapy may have modest efficacy in KRAS-mutant A549 cells—but not in PIK3CA-mutant models—potentially reflecting co-occurring genetic alterations or other context-dependent factors. Tumor volume reduction was more pronounced in the alpelisib and CQ co-treated groups than in those treated with alpelisib alone (Fig. 4E and F). Combination treatment did not adversely affect the overall health of the mice, as indicated by their consistent body weight measurements, which were recorded every two days throughout the study (Fig. 4G and H).

To comprehensively understand the pathways and mechanisms involved in the xenograft mice co-treated with alpelisib and CQ, we analyzed the expression of proteins associated with the PI3K/AKT/mTOR pathway, autophagy, tumorigenesis, and apoptosis within the xenograft tumor tissues. Consistent with the *in vitro* experiments, the immunoblot analysis demonstrated inhibition of both the PI3K/AKT/mTOR pathway and autophagy, along with increased CASP3 cleavage in A549 or H460 xenograft tumors co-treated with alpelisib and CQ (Fig. 5A–D; Fig. S6A and B). Moreover, protein levels of EGFR and Ras were significantly reduced in the H460 xenograft tumors co-treated with alpelisib and CQ, mirroring the effects observed *in vitro* (Fig. 5C and D; Fig. S6B). These findings indicate that the combination produces more profound signaling suppression in H460 xenografts, consistent with preferential efficacy in PI3K–mutant tumors. Collectively, these results underscore the potential of combining CQ with alpelisib to enhance chemotherapeutic efficacy as a promising therapeutic strategy for treating NSCLC with or without PI3K mutations.

4. Discussion

Alterations in the PI3K pathway are commonly observed in various cancers, and PI3K–targeted therapies are widely used in clinical practice. However, monotherapy with PI3K inhibitors has shown limited effectiveness and notable side effects in cancer patients. Therefore, treatments that combine PI3K inhibitors with other mechanism-related activators/inhibitors are being investigated in both clinical and laboratory settings. For instance, the combination of alpelisib and olaparib, a PARP inhibitor, demonstrated superior effects to either drug alone in epithelial ovarian cancer [9]. Zhong et al. overcame the limited effectiveness of pictilisib, an orally bioavailable class I PI3K inhibitor, by combining PI3K and MEK inhibitors [38]. Recently, combined treatment with gefitinib and BYL719 has shown promise in overcoming the EGFR tyrosine kinase inhibitor resistance caused by PI3K/AKT activation in NSCLC cells [39]. In this study, we examined the therapeutic potential of combining alpelisib with autophagy inhibitors to improve treatment outcomes in NSCLC experimental models.

Autophagy plays a dual role in cancer, both preventing tumor formation and supporting the survival of cancer cells under growth-limiting conditions. Recent studies have shown that drug-induced autophagy can lead to chemotherapy failure and the development of chemoresistance [40]. In ovarian cancer cells, autophagy acts as a compensatory mechanism to evade cell death after treatment with taselisib, a PI3K inhibitor [41]. Therefore, blocking abnormal autophagy induction is an effective method for enhancing antitumor effects. CQ, an autophagy inhibitor, has previously been used to investigate the combined effects of anticancer agents and autophagy inhibitors [42]. In this study, we found that alpelisib treatment dose- and time-dependently activated autophagy and suppressed tumor cell growth, as evidenced by changes in protein expression and cell viability assays. Furthermore, combination treatment with alpelisib and various autophagy inhibitors demonstrated more potent suppression of cancer cell growth than alpelisib alone in NSCLC cell lines, including A549 and H460, and xenograft mouse models. Similar findings by Cocco et al. showed that combined administration of PI3K inhibitors and CQ enhanced anticancer effects in triple-negative breast cancer models [43]. Thus, inhibiting autophagy in combination with alpelisib treatment could have potential antitumor effects in NSCLC.

Apoptosis, a programmed cell death process, is essential for the development and survival of organisms. Consequently, the activation of apoptosis is a major target for cancer therapy, although only a few anticancer drugs designed to inhibit BCL-2 family members have been FDA-approved [44]. Recent studies have explored the induction of

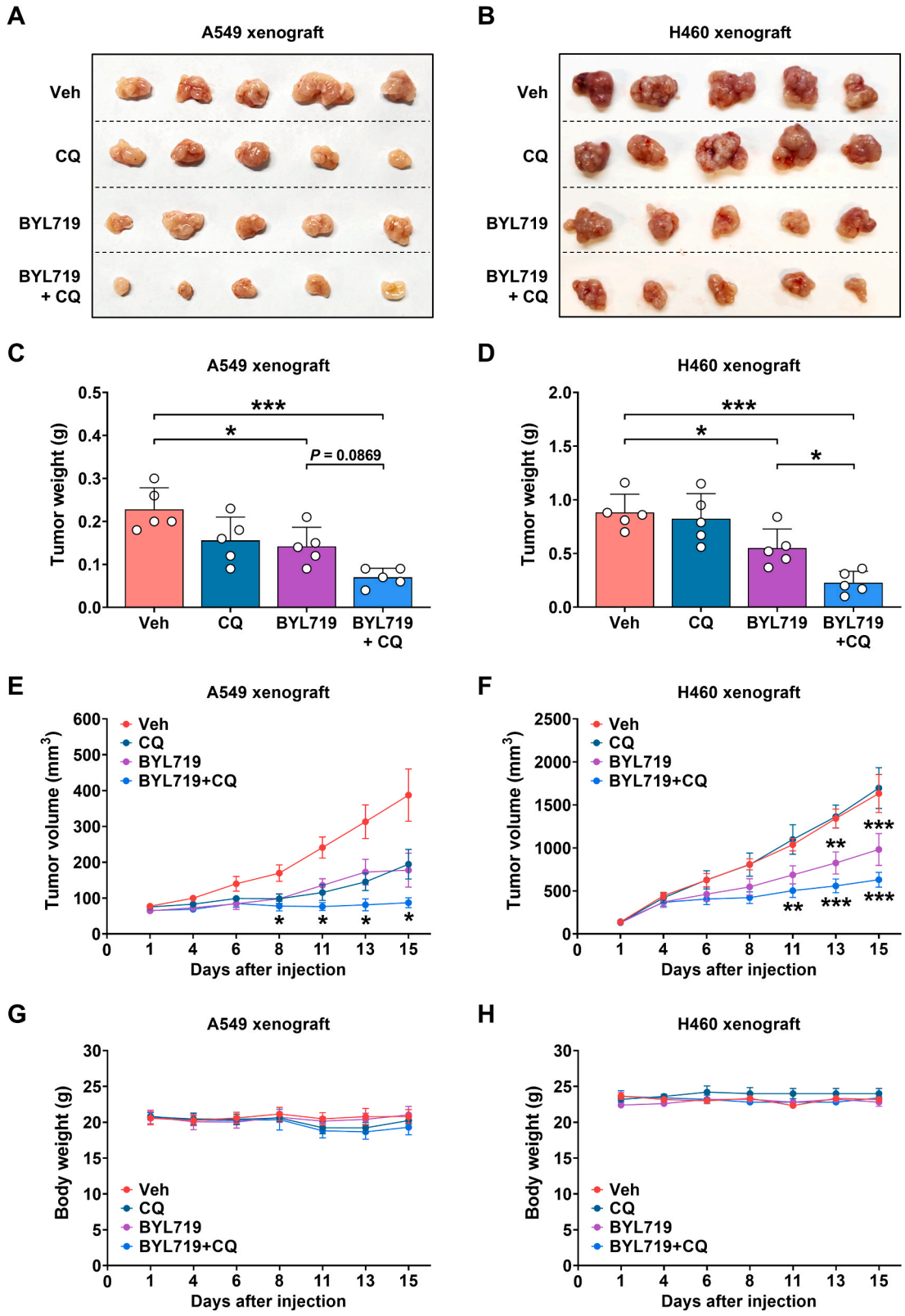

Fig. 4. Alpelisib combined with chloroquine strongly suppresses tumor growth in xenograft mouse models. A–B Gross images of tumors isolated from the vehicle (Veh)-treated group (n = 5), alpelisib (BYL719; 25 mg/kg)-treated group (n = 5), chloroquine (CQ; 30 mg/kg)-treated group (n = 5), and BYL719 +CQ co-treated group (n = 5) of A549 (A) and H460 (B) xenograft mice. C–D Tumor weights in A549 (C) and H460 (D) xenograft mice were measured at the end of the experiment. E–F Tumor volumes in A549 (E) and H460 (F) xenograft mice were calculated as: V = (length × width^2)/2. G–H The body weights of A549 (G) and H460 (H) xenograft mice were measured three times a week for 15 days. All data are shown as the mean ± SD. *p < 0.05, **p < 0.01, and ***p < 0.001 by one-way ANOVA (C and D) and two-way ANOVA (E–H) with Tukey's test.

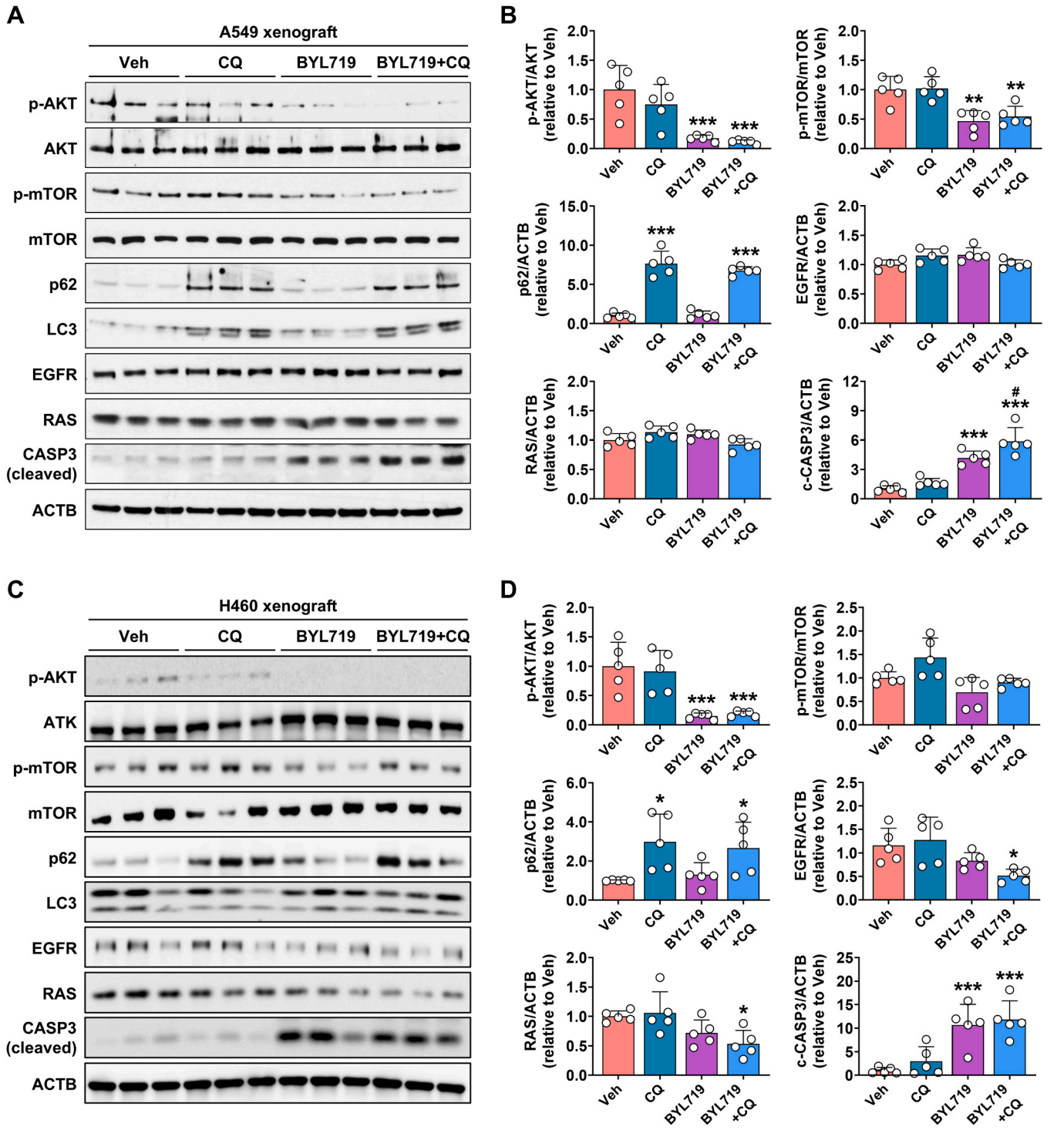

Fig. 5. Alpelisib combined with chloroquine reduces the expression of EGFR and Ras in xenograft mouse models. A–D Immunoblotting analysis of autophagy (p62 and LC3), the PI3K/AKT/mTOR pathway (p-AKT and p-mTOR), tumorigenesis (EGFR and RAS), and apoptosis (cleaved caspase-3) in the vehicle (Veh)-treated group (n = 5), alpelisib (BYL719; 25 mg/kg)-treated group (n = 5), chloroquine (CQ; 30 mg/kg)-treated group (n = 5), and BYL719 +CQ co-treated group (n = 5) of A549 (A) and H460 (C) xenograft mice. The quantitative analyses are summarized in (B and D). Band intensity was determined by densitometry and normalized to β-actin (ACTB) band intensity. All data are shown as the mean ± SD. *p < 0.05, **p < 0.01, and ***p < 0.001 by one-way ANOVA with Tukey's test.

apoptosis using existing anticancer drugs and inhibitors/activators of various mechanisms. For instance, the combination of apatinib, an anti-angiogenic agent, and doxorubicin increased apoptosis induction in triple-negative breast cancer, compared with doxorubicin monotherapy [45]. Treating gastric cancer cells with biosynthetic silver nanoparticles in combination with 5-fluorouracil, a common chemotherapeutic agent, suppressed gastric cancer cell growth by generating reactive oxygen species and promoting apoptosis [46]. Furthermore, miR-323a was found to block the acquisition of gefitinib resistance by inducing apoptosis [47]. In this study, the combination of alpelisib and CQ increased apoptosis in both *in vitro* and *in vivo* models, compared with alpelisib monotherapy. Our data suggest that combining alpelisib and CQ reduced cancer cell viability by enhancing apoptosis.

As shown in previous cancer research, the EGF receptor plays a

critical role in regulating cancer cell proliferation and survival through its effects on various downstream pathways, including the PI3K/AKT/mTOR, JAK/STAT3, and Ras/Raf/MEK/ERK pathways. Ras, a downstream protein of EGFR, is an important target for cancer treatment, and several drugs targeting Ras are under development. Sotorasib (AMG510) has recently been approved by the FDA for the treatment of specific RAS-mutated NSCLC [48]. A combination of EGFR and MEK inhibitors, such as WZ4002, has been shown to enhance chemosensitivity in lung cancer patients with EGFR mutations [49]. Our data show that co-treatment with alpelisib and CQ markedly decreased phosphorylated EGFR in both A549 and H460 cells, whereas reductions in total EGFR and total Ras were largely restricted to PI3K–mutant H460 cells. Although PI3K inhibition alone can elicit compensatory receptor tyrosine kinase (RTK) upregulation and resistance [50,51], the alpelisib–CQ combination in H460 uniquely lowered total EGFR and Ras abundance, suggesting an RTK 'down-scaling' mechanism that may limit adaptive resistance—an effect not observed in KRAS-mutant A549 cells. In contrast to sotorasib, which targets KRAS G12C yet remains vulnerable to RTK-mediated pathway reactivation [52,53], our combination appears to reduce upstream receptor and Ras levels, potentially explaining its selective activity in PI3K–mutant tumors.

The lack of a synergistic effect on STAT3 was unexpected given its position downstream of EGFR; however, STAT3 signaling in NSCLC can be sustained via JAK kinases and cytokine pathways [54,55], which may account for its relative insensitivity to PI3K–autophagy co-targeting. Collectively, these findings suggest that the therapeutic efficacy of alpelisib plus CQ is mediated predominantly through PI3K/AKT/mTOR and EGFR/Ras suppression rather than the JAK/STAT3 axis.

The preferential EGFR/Ras down-regulation in PI3K–mutant H460—but not KRAS-mutant A549—further underscores mutation-specific dependencies: PI3K–mutant cells appear more susceptible to RTK down-scaling that augments PI3K blockade [56], whereas oncogenic KRAS can maintain downstream signaling despite reduced receptor levels, constraining the benefit of this combination. This highlights the importance of genetic context in the application of PI3K–targeted therapies.

This result suggests that combination treatment with alpelisib and CQ might be mechanistically effective in PI3K–mutated cells. Although some research has reported that EGFR and Ras can regulate autophagy activation by modulating ATG5 and ATG7 expression and the interaction between Bcl2/Mcl1 and Beclin1 [57], our results indicate that co-treatment with alpelisib and CQ did not affect autophagy modulation through EGFR and Ras. However, it did exhibit an inhibitory effect on tumor cell growth by regulating the expression of the EGFR and Ras proteins. The JAK/STAT3 pathway, another one of EGFR's downstream pathways, is a well-known mediator of cell proliferation and autophagy inhibition [58]. Our results show no additional reduction in STAT3 expression when alpelisib was combined with CQ treatment, suggesting that the JAK/STAT3 pathway might not be a major mechanism of action for this combined treatment. Therefore, the combination of alpelisib and CQ suppressed tumor cell growth by regulating the expression of the EGFR and Ras proteins, rather than by affecting the autophagic changes associated with EGFR and Ras in PI3K mutation cells.

In summary, Alpelisib selectively inhibits the PI3K/AKT/mTOR signaling pathway, reducing tumor growth in NSCLC. However, this inhibition triggers autophagy, which helps tumor cells survive and develop resistance. Co-treatment with CQ, an autophagy inhibitor, enhances tumor cell death and reduces this resistance. Additionally, in PI3K–mutated human lung cancer, alpelisib leads to AKT inactivation, activating ERK through negative crosstalk with Raf. This activated ERK inhibits receptor tyrosine kinases (RTKs), including EGFR and Ras, thus decreasing tumor cell proliferation and promoting apoptosis (Fig. 6). Consequently, our findings demonstrate that combining alpelisib and CQ induces apoptosis in NSCLC cells, as evidenced by the increased expression of apoptosis-related proteins and a higher number of apoptotic cells, compared with alpelisib monotherapy. Notably, the synergistic effects of alpelisib and CQ co-treatment were particularly effective in PI3K–mutated cells. Therefore, our results provide

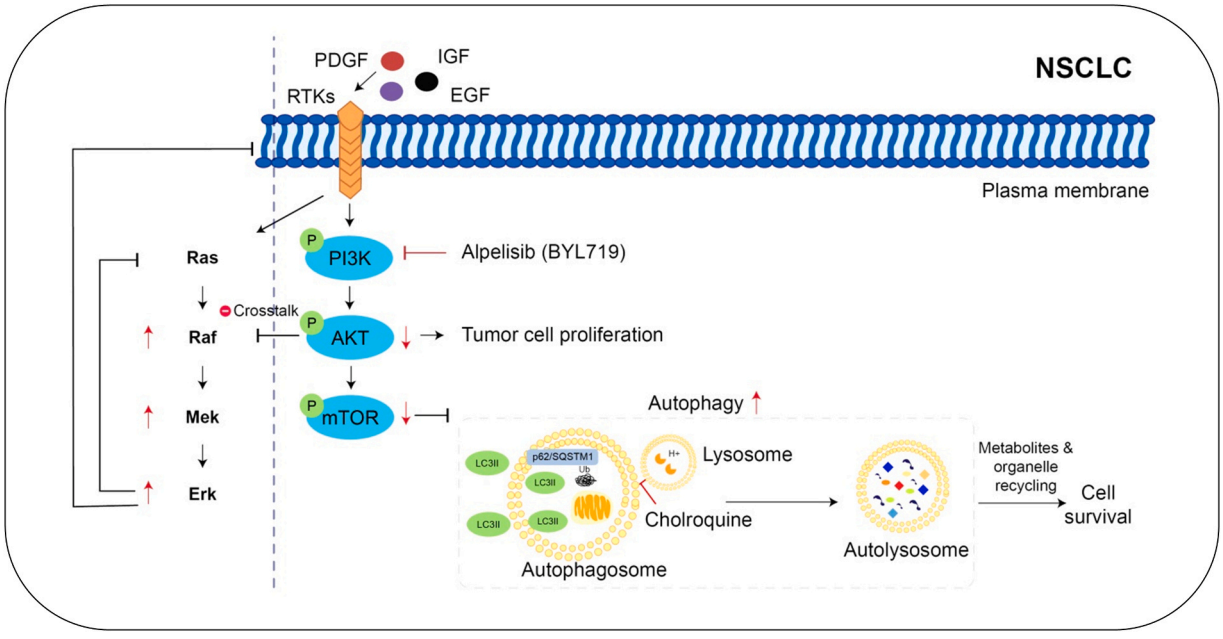

Fig. 6. Schematic diagram illustrating the effects of co-treatment with alpelisib and chloroquine in human NSCLC cells. Alpelisib (BYL719) selectively inhibits the PI3K/AKT/mTOR signaling pathway, thereby suppressing tumor growth in NSCLC. This inhibition activates autophagy as a compensatory mechanism, enhancing tumor cell survival and ultimately contributing to the development of resistance against alpelisib. Co-treatment with CQ, an established autophagy inhibitor, notably induces tumor cell death and mitigates the resistance conferred by autophagy. Furthermore, in PI3K–mutated human lung cancer, alpelisib-induced AKT inactivation leads to the activation of ERK through negative crosstalk with Raf. This activated ERK subsequently inhibits the expression of upstream receptor tyrosine kinases (RTKs), likely including EGFR, and Ras via negative feedback regulation, thereby suppressing tumor cell proliferation and promoting apoptosis. This schematic diagram was created by Editage (Cactus Communications, Seoul, Republic of Korea).

compelling evidence that combining alpelisib and CQ could be an effective treatment approach for PI3K–mutated NSCLC.

Despite the promising findings, several limitations warrant consideration for clinical translation. Alpelisib—while effective in PIK3CA-mutant cancers—is associated with class-specific toxicities such as hyperglycemia and rash [59]. These events are increasingly manageable with glucose monitoring, early metformin initiation, and supportive dermatologic care [60], yet tolerability remains a concern. Adding CQ may further complicate safety, given reports of gastrointestinal intolerance, dermatologic reactions, and rare cardiotoxicity [61]; nonetheless, oncology trials indicate that CQ can be administered safely at clinically relevant doses with appropriate monitoring. A further limitation is that CQ is not a potent autophagy inhibitor relative to next-generation lysosomal agents (e.g., Lys05, DC661), which show superior preclinical activity but remain investigational [62,63]. Finally, benefit from PI3Kα inhibition is enriched in PIK3CA-mutant tumors, underscoring the need for patient selection. Incorporation of validated PIK3CA testing—already standard in breast cancer [59]—will likely be essential to maximize the clinical impact of alpelisib combined with autophagy inhibition in NSCLC.

CRediT authorship contribution statement

Gwangbin Lee: Validation, Investigation. **Dasom Jung:** Validation, Investigation. **Min Hwang:** Validation, Investigation. **Shinwon Kang:** Writing – review & editing. **Byoung Yong Shim:** Writing – review & editing, Supervision, Funding acquisition, Conceptualization. **Chandani Shrestha:** Writing – original draft, Investigation, Formal analysis. **Jiyoon Kim:** Writing – review & editing, Supervision, Project administration, Funding acquisition, Conceptualization. **Tae Woo Kim:** Methodology, Investigation, Formal analysis. **Sang-Bin Lee:** Methodology, Investigation, Formal analysis. **Hyung Soon Park:** Writing – review & editing, Conceptualization. **Hyunho Kim:** Writing – review & editing, Conceptualization. **Ho Jung An:** Writing – review & editing, Conceptualization. **Dongwoo Chae:** Writing – review & editing, Supervision, Funding acquisition, Conceptualization. **Jinyoung Kim:** Writing – original draft, Methodology, Investigation, Formal analysis.

Declaration of Competing Interest

The authors declare that they have no known competing financial interests or personal relationships that could have appeared to influence the work reported in this paper.

Acknowledgements

This study was supported by the National Research Foundation of Korea (NRF) funded by the Ministry of Science and ICT, Republic of Korea (2019R1F1A1062889 and RS-2024-00405790) and Yuhan Corporation.

Appendix A. Supporting information

Supplementary data associated with this article can be found in the online version at doi:10.1016/j.biopha.2025.118620.

Data availability

Data will be made available on request.

References

[1] R.L. Siegel, A.N. Giaquinto, A. Jemal, Cancer statistics, 2024, CA Cancer J. Clin. 74 (1) (2024) 12–49.
[2] D.S. Jeon, H.C. Kim, S.H. Kim, T.J. Kim, H.K. Kim, M.H. Moon, K.S. Beck, Y.G. Suh, C. Song, J.S. Ahn, J.E. Lee, J.U. Lim, J.H. Jeon, K.W. Jung, C.Y. Jung, J.S. Cho, Y. D. Choi, S.S. Hwang, C.M. Choi, Five-Year overall survival and prognostic factors in patients with lung cancer: results from the Korean association of lung cancer registry (KALC-R) 2015, Cancer Res Treat. 55 (1) (2023) 103–111.
[3] Q. Guo, L. Liu, Z. Chen, Y. Fan, Y. Zhou, Z. Yuan, W. Zhang, Current treatments for non-small cell lung cancer, Front. Oncol. 12 (2022) 945102.
[4] V.S. Sabine, C. Crozier, C.L. Brookes, C. Drake, T. Piper, C.J. van de Velde, A. Hasenburg, D.G. Kieback, C. Markopoulos, L. Dirix, C. Seynaeve, D.W. Rea, J. M. Bartlett, Mutational analysis of PI3K/AKT signaling pathway in tamoxifen exemestane adjuvant multinational pathology study, J. Clin. Oncol. 32 (27) (2014) 2951–2958.
[5] Y. Samuels, L.A. Diaz Jr., O. Schmidt-Kittler, J.M. Cummins, L. Delong, I. Cheong, C. Rago, D.L. Huso, C. Lengauer, K.W. Kinzler, B. Vogelstein, V.E. Velculescu, Mutant PIK3CA promotes cell growth and invasion of human cancer cells, Cancer Cell 7 (6) (2005) 561–573.
[6] Y.H. Fan, H.W. Ding, D. Kim, J.Y. Liu, J.Y. Hong, Y.N. Xu, D. Wang, X.S. Yang, S. K. Lee, The PI3Kα inhibitor DFX24 suppresses tumor growth and metastasis in non-small cell lung cancer via ERK inhibition and EPHB6 reactivation, Pharm. Res. 160 (2020) 105147.
[7] R. Shi, M. Li, V. Raghavan, S. Tam, M. Cabanero, N.A. Pham, F.A. Shepherd, N. Moghal, M.S. Tsao, Targeting the CDK4/6-Rb pathway enhances response to PI3K inhibition in PIK3CA-Mutant lung squamous cell carcinoma, Clin. Cancer Res. 24 (23) (2018) 5990–6000.
[8] C.P. Hedges, J. Boix, J.K. Jaiswal, B. Shetty, P.R. Shepherd, T.L. Merry, Efficacy of providing the PI3K p110α inhibitor BYL719 (Alpelisib) to Middle-Aged mice in their diet, Biomolecules 11 (2) (2021).
[9] P.A. Konstantinopoulos, W.T. Barry, M. Birrer, S.N. Westin, K.A. Cadoo, G. I. Shapiro, E.L. Mayer, R.E.O. Cearbhaill, R.L. Coleman, B. Kochupurakkal, C. Whalen, J. Curtis, S. Farooq, W. Luo, J. Eismann, M.K. Buss, C. Aghajanian, G. B. Mills, S. Palakurthi, P. Kirschmeier, J. Liu, L.C. Cantley, S.H. Kaufmann, E. M. Swisher, A.D.D. Andrea, E. Winer, G.M. Wulf, U.A. Matulonis, Olaparib and α-specific PI3K inhibitor alpelisib for patients with epithelial ovarian cancer: a dose-escalation and dose-expansion phase 1b trial, Lancet Oncol. 20 (4) (2019) 570–580.
[10] K.J. Kim, J.W. Kim, J.H. Sung, K.J. Suh, J.Y. Lee, S.H. Kim, J.O. Lee, J.W. Kim, Y. J. Kim, J.H. Kim, S.M. Bang, J.S. Lee, H.K. Kim, K.W. Lee, PI3K–targeting strategy using alpelisib to enhance the antitumor effect of paclitaxel in human gastric cancer, Sci. Rep. 10 (1) (2020) 12308.
[11] J.F. Vansteenkiste, J.-L. Canon, F. De Braud, F. Grossi, T. De Pas, J.E. Gray, W.-C. Su, E. Felip, H. Yoshioka, C. Gridelli, Safety and efficacy of buparlisib (BKM120) in patients with PI3K pathway-activated non-small cell lung cancer: results from the phase II BASALT-1 study, J. Thorac. Oncol. 10 (9) (2015) 1319–1327.
[12] A.R. Lim, B. Kim, J.H. Kim, M.H. Hyun, K.H. Park, Y.H. Kim, S. Lee, Phase ib and pharmacokinetics study of alpelisib, a PIK3CA inhibitor, and capecitabine in patients with advanced solid tumors, Front. Oncol. 14 (2024), 1390452.
[13] S. Heavey, S. Cuffe, S. Finn, V. Young, R. Ryan, S. Nicholson, N. Leonard, N. McVeigh, M. Barr, K.O. Byrne, In pursuit of synergy: an investigation of the PI3K/mTOR/MEK co-targeted inhibition strategy in NSCLC, Oncotarget 7 (48) (2016) 79526.
[14] T. Kimura, Y. Takabatake, A. Takahashi, Y. Isaka, Chloroquine in cancer therapy: a double-edged sword of autophagy, Cancer Res. 73 (1) (2013) 3–7.
[15] R. Amaravadi, A.C. Kimmelman, E. White, Recent insights into the function of autophagy in cancer, Genes Dev. 30 (17) (2016) 1913–1930.
[16] F. Liu, Y. Shang, S.-z Chen, Chloroquine potentiates the anti-cancer effect of lidamycin on non-small cell lung cancer cells in vitro, Acta Pharmacol. Sin. 35 (5) (2014) 645–652.
[17] J. Sotelo, E. Briceño, M.A. López-González, Adding chloroquine to conventional treatment for glioblastoma multiforme: a randomized, double-blind, placebo-controlled trial, Ann. Intern. Med. 144 (5) (2006) 337–343.
[18] E. White, The role for autophagy in cancer, J. Clin. Investig. 125 (1) (2015) 42–46.
[19] J.Y. Guo, H.Y. Chen, R. Mathew, J. Fan, A.M. Strohecker, G. Karsli-Uzunbas, J. J. Kamphorst, G. Chen, J.M. Lemons, V. Karantza, H.A. Coller, R.S. Dipaola, C. Gelinas, J.D. Rabinowitz, E. White, Activated ras requires autophagy to maintain oxidative metabolism and tumorigenesis, Genes Dev. 25 (5) (2011) 460–470.
[20] S. Wang, J. Li, Y. Du, Y. Xu, Y. Wang, Z. Zhang, Z. Xu, Y. Zeng, X. Mao, B. Cao, The class I PI3K inhibitor S14161 induces autophagy in malignant blood cells by modulating the beclin 1/Vps34 complex, J. Pharm. Sci. 134 (4) (2017) 197–202.
[21] T.-C. Chou, Drug combination studies and their synergy quantification using the Chou-Talalay method, Cancer Res. 70 (2) (2010) 440–446.
[22] P. Castel, E. Toska, J.A. Engelman, M. Scaltriti, The present and future of PI3K inhibitors for cancer therapy, Nat. Cancer 2 (6) (2021) 587–597.
[23] E.L.H. Leung, L.X. Luo, Z.Q. Liu, V.K.W. Wong, L.L. Lu, Y. Xie, N. Zhang, Y.Q. Qu, X.X. Fan, Y. Li, M. Huang, D.K. Xiao, J. Huang, Y.L. Zhou, J.X. He, J. Ding, X.J. Yao, D.C. Ward, L. Liu, Inhibition of KRAS-dependent lung cancer cell growth by deltarasin: blockage of autophagy increases its cytotoxicity, Cell Death Dis. 9 (2) (2018) 216.
[24] S. Heavey, S. Cuffe, S. Finn, V. Young, R. Ryan, S. Nicholson, N. Leonard, N. McVeigh, M. Barr, K.O. Byrne, K. Gately, In pursuit of synergy: an investigation of the PI3K/mTOR/MEK co-targeted inhibition strategy in NSCLC, Oncotarget 7 (48) (2016) 79526–79543.
[25] S. Cocco, A. Leone, M. Piezzo, R. Caputo, V. Di Lauro, F. Di Rella, G. Fusco, M. Capozzi, G.D. Gioia, A. Budillon, M. De Laurentiis, Targeting autophagy in breast cancer, Int. J. Mol. Sci. 21 (21) (2020).
[26] S.C.E. Wright, N. Vasilevski, V. Serra, J. Rodon, P.J.A. Eichhorn, Mechanisms of resistance to PI3K inhibitors in cancer: adaptive responses, drug tolerance and cellular plasticity, Cancers 13 (7) (2021).

[27] Z.N. Lei, Z.X. Wu, S. Dong, D.H. Yang, L. Zhang, Z. Ke, C. Zou, Z.S. Chen, Chloroquine and hydroxychloroquine in the treatment of malaria and repurposing in treating COVID-19, Pharm. Ther. 216 (2020) 107672.
[28] J.E. Jonkman, J.A. Cathcart, F. Xu, M.E. Bartolini, J.E. Amon, K.M. Stevens, P. Colarusso, An introduction to the wound healing assay using live-cell microscopy, Cell Adh Migr. 8 (5) (2014) 440–451.
[29] D. Wlodkowic, W. Telford, J. Skommer, Z. Darzynkiewicz, Apoptosis and beyond: cytometry in studies of programmed cell death, Methods Cell Biol. 103 (2011) 55–98.
[30] M.M. Sadeghipour, S.A. Torabizadeh, M.N. Karimabad, The Glucose-Regulated Protein78 (GRP78) in the unfolded protein response (UPR) pathway: a potential therapeutic target for breast cancer, AntiCancer Agents Med. Chem. AntiCancer Agents 23 (5) (2023) 505–524.
[31] H. Li, X. Zhu, F. Fang, D. Jiang, L. Tang, Down-regulation of GRP78 enhances apoptosis via CHOP pathway in retinal ischemia-reperfusion injury, Neurosci. Lett. 575 (2014) 68–73.
[32] T. Suzuki, J. Lu, M. Zahed, K. Kita, N. Suzuki, Reduction of GRP78 expression with siRNA activates unfolded protein response leading to apoptosis in HeLa cells, Arch. Biochem. Biophys. 468 (1) (2007) 1–14.
[33] T. Mizukami, N. Izawa, T.E. Nakajima, Y. Sunakawa, Targeting EGFR and RAS/RAF signaling in the treatment of metastatic colorectal cancer: from current treatment strategies to future perspectives, Drugs 79 (6) (2019) 633–645.
[34] H.Y.K. Yip, S.-Y. Shin, A. Chee, C.-S. Ang, F.J. Rossello, L.H. Wong, L.K. Nguyen, A. Papa, Integrative modeling uncovers p21-driven drug resistance and prioritizes therapies for PIK3CA-mutant breast cancer, NPJ Precis. Oncol. 8 (1) (2024) 20.
[35] A.B. Nair, S. Jacob, A simple practice guide for dose conversion between animals and human, J. Basic Clin. Pharm. 7 (2) (2016) 27.
[36] J. Shen, H. Zheng, J. Ruan, W. Fang, A. Li, G. Tian, X. Niu, S. Luo, P. Zhao, Autophagy inhibition induces enhanced proapoptotic effects of ZD6474 in glioblastoma, Br. J. Cancer 109 (1) (2013) 164–171.
[37] C. Verbaanderd, H. Maes, M.B. Schaaf, V.P. Sukhatme, P. Pantziarka, V. Sukhatme, P. Agostinis, G. Bouche, Repurposing drugs in oncology (ReDO)—chloroquine and hydroxychloroquine as anti-cancer agents, ecancermedicalscience 11 (2017) 781.
[38] H. Zhong, C. Sanchez, D. Spitzer, S. Plambeck-Suess, J. Gibbs, W.G. Hawkins, D. Denardo, F. Gao, R.A. Pufahl, A.C. Lockhart, M. Xu, D. Linehan, J. Weber, A. Wang-Gillam, Synergistic effects of concurrent blockade of PI3K and MEK pathways in pancreatic cancer preclinical models, PLoS One 8 (10) (2013) e77243.
[39] Y. Yu, Z. Xiao, C. Lei, C. Ma, L. Ding, Q. Tang, Y. He, Y. Chen, X. Chang, Y. Zhu, H. Zhang, BYL719 reverses gefitinib-resistance induced by PI3K/AKT activation in non-small cell lung cancer cells, BMC Cancer 23 (1) (2023) 732.
[40] S. Liu, X. Li, Autophagy inhibition enhances sensitivity of endometrial carcinoma cells to paclitaxel, Int J. Oncol. 46 (6) (2015) 2399–2408.
[41] J. Zorea, M. Prasad, L. Cohen, N. Li, R. Schefzik, S. Ghosh, B. Rotblat, B. Brors, M. Elkabets, IGF1R upregulation confers resistance to isoform-specific inhibitors of PI3K in PIK3CA-driven ovarian cancer, Cell Death Dis. 9 (10) (2018) 944.
[42] T. Kimura, Y. Takabatake, A. Takahashi, Y. Isaka, Chloroquine in cancer therapy: a double-edged sword of autophagy, Cancer Res 73 (1) (2013) 3–7.
[43] S. Cocco, A. Leone, M.S. Roca, R. Lombardi, M. Piezzo, R. Caputo, C. Ciardiello, S. Costantini, F. Bruzzese, M.J. Sisalli, A. Budillon, M. De Laurentiis, Inhibition of autophagy by chloroquine prevents resistance to PI3K/AKT inhibitors and potentiates their antitumor effect in combination with paclitaxel in triple negative breast cancer models, J. Transl. Med. 20 (1) (2022) 290.
[44] B.A. Carneiro, W.S. El-Deiry, Targeting apoptosis in cancer therapy, Nat. Rev. Clin. Oncol. 17 (7) (2020) 395–417.
[45] D. Tang, J. Ma, Z. Chu, X. Wang, W. Zhao, Q. Zhang, Apatinib-induced NF-κB inactivation sensitizes triple-negative breast cancer cells to doxorubicin, Am. J. Transl. Res. 12 (7) (2020) 3741–3753.
[46] J. Yuan, S.U. Khan, J. Luo, Y. Jiang, Y. Yang, J. Yan, Q. Tong, Biosynthetic silver nanoparticles inhibit the malignant behavior of gastric cancer cells and enhance the therapeutic effect of 5-Fluorouracil by promoting intracellular ROS generation and apoptosis, Pharmaceutics 14 (10) (2022).
[47] Y. Zhang, S. Liang, B. Xiao, J. Hu, Y. Pang, Y. Liu, J. Yang, J. Ao, L. Wei, X. Luo, MiR-323a regulates ErbB3/EGFR and blocks gefitinib resistance acquisition in colorectal cancer, Cell Death Dis. 13 (3) (2022) 256.
[48] H.A. Blair, Sotorasib: first approval, Drugs 81 (13) (2021) 1573–1579.
[49] D. Ercan, C. Xu, M. Yanagita, C.S. Monast, C.A. Pratilas, J. Montero, M. Butaney, T. Shimamura, L. Sholl, E.V. Ivanova, M. Tadi, A. Rogers, C. Repellin, M. Capelletti, O. Maertens, E.M. Goetz, A. Letai, L.A. Garraway, M.J. Lazzara, N. Rosen, N. S. Gray, K.K. Wong, P.A. Jänne, Reactivation of ERK signaling causes resistance to EGFR kinase inhibitors, Cancer Discov. 2 (10) (2012) 934–947.
[50] S. Chandarlapaty, A. Sawai, M. Scaltriti, V. Rodrik-Outmezguine, O. Grbovic-Huezo, V. Serra, P.K. Majumder, J. Baselga, N. Rosen, AKT inhibition relieves feedback suppression of receptor tyrosine kinase expression and activity, Cancer Cell 19 (1) (2011) 58–71.
[51] V. Serra, M. Scaltriti, L. Prudkin, P.J. Eichhorn, Y.H. Ibrahim, S. Chandarlapaty, B. Markman, O. Rodriguez, M. Guzman, S. Rodriguez, PI3K inhibition results in enhanced HER signaling and acquired ERK dependency in HER2-overexpressing breast cancer, Oncogene 30 (22) (2011) 2547–2557.
[52] S.R. Punekar, V. Velcheti, B.G. Neel, K.-K. Wong, The current state of the art and future trends in RAS-targeted cancer therapies, Nat. Rev. Clin. Oncol. 19 (10) (2022) 637–655.
[53] M.M. Awad, S. Liu, I.I. Rybkin, K.C. Arbour, J. Dilly, V.W. Zhu, M.L. Johnson, R. S. Heist, T. Patil, G.J. Riely, Acquired resistance to KRASG12C inhibition in cancer, N. Engl. J. Med. 384 (25) (2021) 2382–2393.
[54] D. Harada, N. Takigawa, K. Kiura, The role of STAT3 in non-small cell lung cancer, Cancers 6 (2) (2014) 708–722.
[55] K. Shien, V.A. Papadimitrakopoulou, D. Ruder, C. Behrens, L. Shen, N. Kalhor, J. Song, J.J. Lee, J. Wang, X. Tang, JAK1/STAT3 activation through a proinflammatory cytokine pathway leads to resistance to molecularly targeted therapy in non–small cell lung cancer, Mol. Cancer Ther. 16 (10) (2017) 2234–2245.
[56] K.W. Song, K.A. Edgar, E.J. Hanan, M. Hafner, J. Oeh, M. Merchant, D. Sampath, M.A. Nannini, R. Hong, L. Phu, RTK-dependent inducible degradation of mutant PI3Kα drives GDC-0077 (Inavolisib) efficacy, Cancer Discov. 12 (1) (2022) 204–219.
[57] X. Ji, H. Ma, Y. Du, role and mechanism of action of LAPTM4B in EGFR-mediated autophagy, Oncol. Lett. 23 (4) (2022) 109.
[58] H.T. Chen, H. Liu, M.J. Mao, Y. Tan, X.Q. Mo, X.J. Meng, M.T. Cao, C.Y. Zhong, Y. Liu, H. Shan, G.M. Jiang, Crosstalk between autophagy and epithelial-mesenchymal transition and its application in cancer therapy, Mol. Cancer 18 (1) (2019) 101.
[59] F. André, E. Ciruelos, G. Rubovszky, M. Campone, S. Loibl, H.S. Rugo, H. Iwata, P. Conte, I.A. Mayer, B. Kaufman, Alpelisib for PIK3CA-mutated, hormone receptor–positive advanced breast cancer, N. Engl. J. Med. 380 (20) (2019) 1929–1940.
[60] S. Nunnery, I. Mayer, Management of toxicity to isoform α-specific PI3K inhibitors, Ann. Oncol. 30 (2019) x21–x26.
[61] F. Askarian, Z. Firoozi, A. Ebadollahi-Natanzi, S. Bahrami, H.-R. Rahimi, A review on the pharmacokinetic properties and toxicity considerations for chloroquine and hydroxychloroquine to potentially treat coronavirus patients, Toxicol. Res. 38 (2) (2022) 137–148.
[62] Q. McAfee, Z. Zhang, A. Samanta, S.M. Levi, X.-H. Ma, S. Piao, J.P. Lynch, T. Uehara, A.R. Sepulveda, L.E. Davis, Autophagy inhibitor Lys05 has single-agent antitumor activity and reproduces the phenotype of a genetic autophagy deficiency, Proc. Natl. Acad. Sci. 109 (21) (2012) 8253–8258.
[63] V.W. Rebecca, M.C. Nicastri, C. Fennelly, C.I. Chude, J.S. Barber-Rotenberg, A. Ronghe, Q. McAfee, N.P. McLaughlin, G. Zhang, A.R. Goldman, PPT1 promotes tumor growth and is the molecular target of chloroquine derivatives in cancer, Cancer Discov. 9 (2) (2019) 220–229.